

Article

Natural Fractures in Carbonate Basement Reservoirs of the Jizhong Sub-Basin, Bohai Bay Basin, China: Key Aspects Favoring Oil Production

Guoping Liu ^{1,2}, Lianbo Zeng ^{1,2,*}, Chunyuan Han ³, Mehdi Ostadhassan ⁴ , Wenya Lyu ^{1,2}, Qiqi Wang ⁵ , Jiangwei Zhu ^{1,2} and Fengxiang Hou ³

¹ State Key Laboratory of Petroleum Resources and Prospecting, China University of Petroleum (Beijing), Beijing 102249, China; liugpzy228@gmail.com (G.L.); wylvwenwen@163.com (W.L.); zhujianghan@gmail.com (J.Z.)

² College of Geosciences, China University of Petroleum (Beijing), Beijing 102249, China

³ PetroChina Huabei Oilfield Company, Cangzhou 062552, China; yjy_hcy@petrochina.com.cn (C.H.); yjy_hfx@petrochina.com.cn (F.H.)

⁴ Department of Petroleum Engineering, University of North Dakota, Grand Forks, ND 58202, USA; mehdi.ostadhassan@gmail.com

⁵ Jackson School of Geosciences, University of Texas at Austin, Austin, TX 78713, USA; wangqiqi@utexas.edu

* Correspondence: lbzeng@sina.com; Tel.: +86-010-8973-1288

Received: 16 August 2020; Accepted: 3 September 2020; Published: 7 September 2020



Abstract: Analysis of natural fractures is essential for understanding the heterogeneity of basement reservoirs with carbonate rocks since natural fractures significantly control key attributes such as porosity and permeability. Based on the observations and analyses of outcrops, cores, borehole image logs, and thin sections from the Mesoproterozoic to Lower Paleozoic in the Jizhong Sub-Basin, natural fractures are found to be abundant in genetic types (tectonic, pressure-solution, and dissolution) in these reservoirs. Tectonic fractures are dominant in such reservoirs, and lithology, mechanical stratigraphy, and faults are major influencing factors for the development of fractures. Dolostones with higher dolomite content are more likely to have tectonic fractures than limestones with higher calcite content. Most tectonic fractures are developed inside mechanical units and terminate at the unit interface at nearly perpendicular or high angles. Also, where a thinner mechanical unit is observed, tectonic fractures are more frequent with a small height. Furthermore, the dominant direction of tectonic fractures is sub-parallel to the fault direction or oblique at a small angle. In addition, integrating diverse characteristics of opening-mode fractures and well-testing data with oil production shows that, in perforated intervals where dolostone and limestone are interstratified or dolostone is the main lithologic composition, fractures are developed well, and the oil production is higher. Moreover, fractures with a larger dip angle have bigger apertures and contribute more to oil production. Collectively, this investigation provides a future reference for understanding the importance of natural fractures and their impact on oil production in the carbonate basement reservoirs.

Keywords: natural fracture; influencing factor; oil production; carbonate rock; basement reservoir; Jizhong Sub-basin

1. Introduction

Basement reservoirs usually refer to traps that accumulate oil and gas in topographic uplifts of basement rocks under unconformities, which are covered by younger sediments [1–4]. Based on their location in topographic uplifts, these reservoirs are divided into weathering crusts and inner

reservoirs [5–7]. Basement rocks include metamorphic rocks and some volcanic and carbonate rocks [4,8–10].

As an important type of unconventional petroleum system for further exploration and development, basement reservoirs are receiving increasing attention worldwide, and hydrocarbons are being exploited from them in areas such as China, North Africa, the USA, and Southeast Asia [1,2,11,12]. Considering recent advancements in production technology and demand for more resources, research to extract oil and gas from the deep inner reservoirs of basements is growing as well [6,13,14]. In the Bohai Bay Basin, basement reservoirs are the primary type of petroleum traps, particularly in the Jizhong Sub-Basin, which is considered as one of the structural units in the Bohai Bay Basin, where 29 out of 43 oil and gas fields are basement reservoirs or related to basement rocks [15]. Volumetric calculations showed proven reserves of 526.83 million tons (3861.66 million bbl) of original oil in place (OOIP) in basement reservoirs, accounting for 51.66% of the total OOIP in the Jizhong Sub-Basin [9]. Carbonate rocks are the primary basement rocks in the Jizhong Sub-basin [16].

Previous studies have shown that primary pores are less in these basement reservoirs, and secondary pores dominate the storage space, mainly composed of dissolution pores and natural fractures [17–19]. Since basement rocks have experienced multiple periods of tectonism and diagenesis, various natural fractures are generally developed, causing significant heterogeneity in such reservoirs [13,20,21]. Like other types of fractured reservoirs, natural fractures are the main flow pathways for hydrocarbons in basement reservoirs [8,12,22,23]. Moreover, natural fractures are a significant component of storage space for petroleum accumulation in these reservoirs as well [24–26], where fractures at different scales can connect pores to control the quality of the reservoir [3,13,27,28].

Despite the vital role that natural fractures play in the reservoir quality as explained above, limited studies are carried out to delineate their significance entirely in basement reservoirs with carbonate rocks. The development of fractures, the main factors affecting their existence, and their contribution to the performance are unclear in such reservoirs and demand further investigation.

This study's primary purpose is to characterize natural fractures and understand their role in oil production in the deep inner reservoirs of carbonate basements in the Jizhong Sub-Basin of the Bohai Bay Basin. Therefore, outcrops, cores, borehole image logs, and thin sections were used in a detailed analysis for fracture characterizations, including orientation, dip angle, height, length, density, aperture, and filling. Based on these, lithology, mechanical stratigraphy, and faults were also analyzed to reveal how they would affect the growth mechanism of fractures. Moreover, the significance of opening-mode fractures on oil production was presented as well. These efforts will enable us to understand the heterogeneity of petrophysical properties and reservoir performances in these basements.

2. Geological Setting

2.1. Location and Structure

The Bohai Bay Basin, which is in the eastern part of China, is a Cenozoic rift basin developed in the basement of the North China Platform [9,29,30] (Figure 1a). The Jizhong Sub-Basin in the northwest is one of the sub-basins in the Bohai Bay Basin. It is distributed in an NNE–SSW direction and covers an area of 32,000 km² (12,355 mile²) [31,32] (Figure 1b). A number of NNE–SSW-oriented depressions, uplifts, and slopes have been developed within the sub-basin. Additionally, two transfer zones—Xushui-Anxin-Wenan and Wuji-Shenxian-Hengshui—are developed in the Jizhong Sub-Basin, near E–W and NW–SE strikes, respectively (Figure 1b). The two transfer zones have divided the sub-basin into three regions: northeast, center, and southwest. The extensional faults formed by multistage tectonic movements are developed in this sub-basin, while grabens and half-grabens, from these faults, have created various topographic uplift structures in this sub-basin [33,34] (Figure 2).

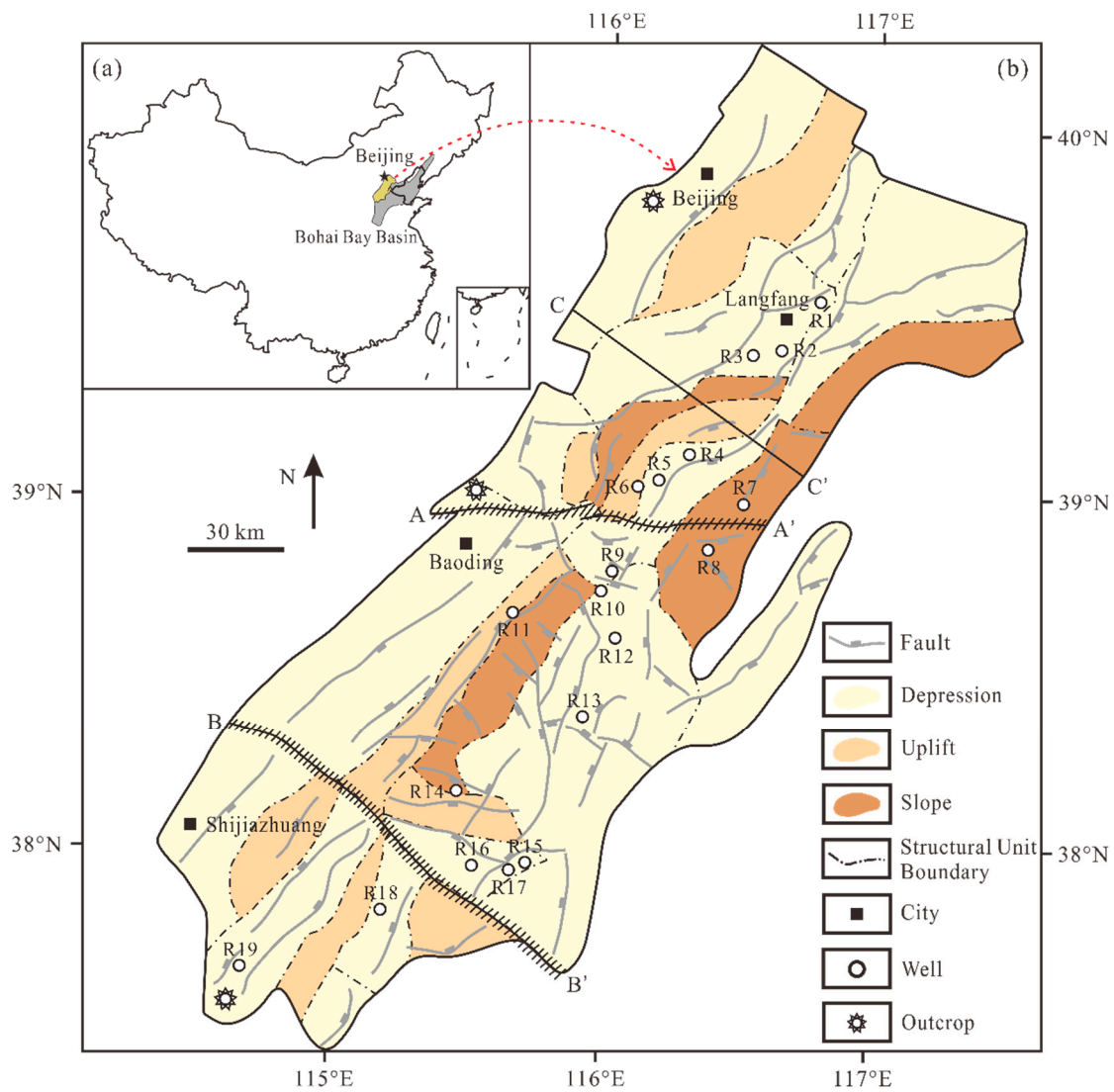


Figure 1. (a) Location of the Jizhong Sub-Basin in the Bohai Bay Basin in China (modified from Zhao et al., 2015) [9]. (b) Map showing the faults, structural units, transfer zones, wells, and outcrops in the Jizhong Sub-Basin (modified from Chang et al., 2016) [35]. The fault data was modified from the Huabei Oilfield database. A-A' is the Xushui-Anxin-Wenan transfer zone, and B-B' is the Wuji-Shenxian-Hengshui transfer zone. C-C' represents the position of the cross-section in Figure 2.

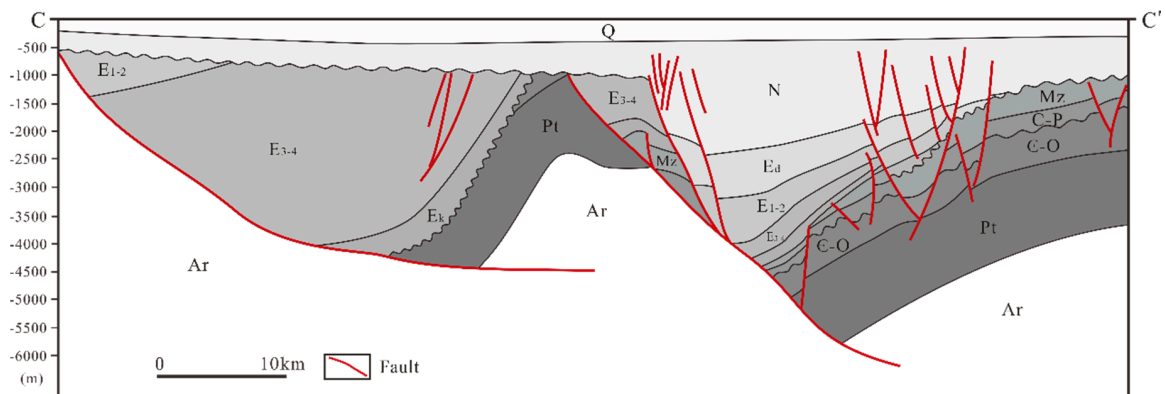


Figure 2. A geological cross-section in the Jizhong Sub-Basin, showing the structural pattern of the strata (modified according to He et al., 2017) [36]. The position of the cross-section is shown by C-C' in Figure 1.

2.2. Stratigraphy

Basement rocks in the Jizhong Sub-Basin are developed in the Archean, Proterozoic, Paleozoic, and Mesozoic from bottom to top (Figures 2 and 3) [19,37]. The Archean and Paleoproterozoic are composed of metamorphic rocks, while the Changcheng, Jixian, and Qingbaikou systems, which are developed in the Mesoproterozoic and Neoproterozoic, are a set of sediments made up of marine carbonate rocks. The Lower Paleozoic develops the Cambrian and Ordovician, which are typical sediments dominated by carbonate rocks of neritic platform facies. The Carboniferous and Permian in the Upper Paleozoic are clastic rocks of continental and transitional facies, where coal-bearing strata are relatively abundant. The Mesozoic is mainly Jurassic and Cretaceous, which are continental clastic rocks containing volcanic rocks. Due to the erosion and intermittent deposition caused by multistage structural uplifts, the Jizhong Sub-Basin strata are absent from the Silurian, Devonian, Early Carboniferous, and Triassic periods [29]. The Cenozoic strata consist of a set of interbedded depositions that are mainly sandstone and mudstone of lacustrine and deltaic facies [38].

The target layer in this study is the basements of carbonate rocks in the Mesoproterozoic, Neoproterozoic, and Lower Paleozoic periods. These basement rocks have undergone complex sedimentation, diagenesis, and tectonism, forming various reservoirs with proven economic hydrocarbon accumulations [39]. Source rocks are mainly dark mudstones of lacustrine facies in the Paleogene, along with coal and dark mudstones of transitional facies in the Carboniferous and Permian periods [40]. These source rocks are often adjacent to the basements, where hydrocarbons have migrated into the reservoir through faults and unconformities [34,41]. It should be noted that these coal and dark mudstones are also good regional caprocks for the carbonate basement reservoirs in this sub-basin. Additionally, many interlayers with high argillaceous content exhibit high-quality caprocks in the inner reservoirs of these basements [36,42]. As a result, combinations of source rocks, reservoirs, and caprocks have created a suitable petroleum system in the carbonate basements of the Jizhong Sub-Basin and have provided great potential for oil and gas exploration and development in this area [9].

2.3. Reservoir

The carbonate rocks that constitute the basement reservoirs in the Mesoproterozoic and Neoproterozoic are mainly dolostone, while in the Lower Paleozoic are dominated by limestone [38]. In these reservoirs, a network of pores and natural fractures have provided the storage space for the economic accumulation of hydrocarbons [17–19]. The pores are mainly secondary and are formed by dissolution, and natural fractures are more frequent and have multiple genetic types. These storage spaces provide favorable conditions for oil and gas accumulation and migration in these reservoirs. The carbonate rocks have an average matrix porosity lower than 12%, while the porosity analysis from cores has shown that samples with a porosity higher than 3% account for more than 70% of all samples [29,43]. The permeability of these basement reservoirs is relatively high, and samples with an air permeability greater than 1 mD account for more than 60% of all measured samples [43].

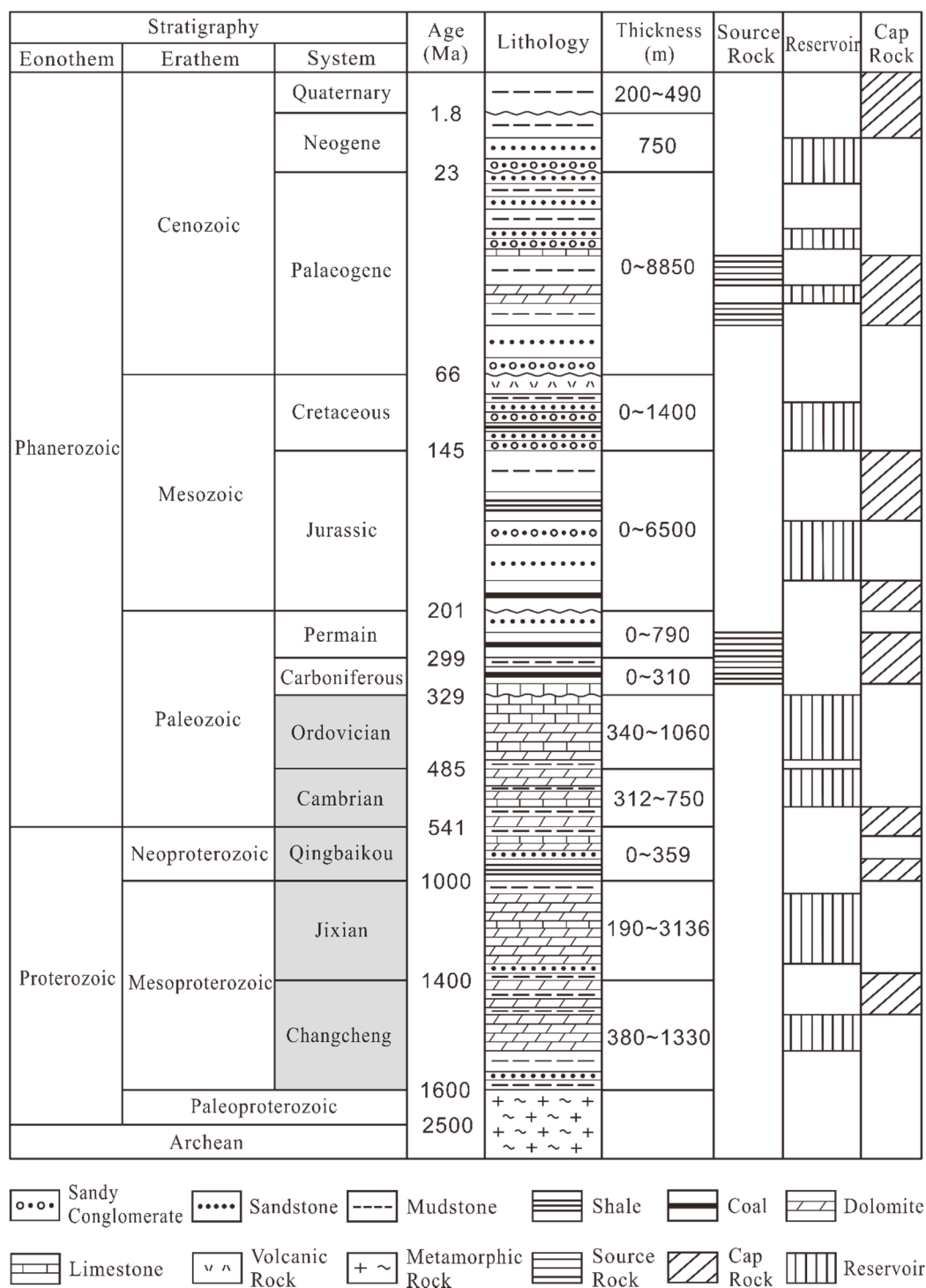


Figure 3. The stratigraphic column of the Jizhong Sub-Basin, showing the major petroleum systems (source rocks, reservoirs, and cap rocks) (modified according to Wu et al., 2011, and Liu et al., 2017) [19,37]. The gray mark in the system is the target layer of this study.

3. Dataset and Methodology

In this investigation, we collected data and samples from outcrops, cores, thin sections, and borehole image logs in the basement reservoirs of carbonate rocks in the Mesoproterozoic to Lower Paleozoic in the Jizhong Sub-Basin of the Bohai Bay Basin in eastern China. The outcrops and subsurface targets are from the same formation and have experienced similar tectonic movements and diageneses [39,44]. Cores and borehole image logs from 19 wells from these basement reservoirs were analyzed as well.

The length of the cores is 123.8 m (406.2 ft). Thin sections are 119 pieces coming from cores. In addition, other useful information such as lithology, fault, perforated interval, and oil production, were collected from the Renqiu Oilfield database and relevant literature. We combined these different sources of data to comprehensively analyze and study the natural fractures in deep inner reservoirs of these basements from macro to micro-scale.

Natural fracture characteristics, including height, length, orientation, dip angle, density, fracture zone, spacing, aperture, and filling, were examined closely from the sources mentioned above. The fracture density in this study refers to the linear density that was measured based on the number of fractures per unit length. The fracture zone is defined as multiple sets of tectonic fractures that are developed in rocks and usually are interwoven into a network, which makes it difficult to measure and count individually. These parameters in outcrops and cores were identified and measured on-site, while in borehole image logs, they were manually picked and interpreted [45,46]. It should be pointed out that in the cores, there are some unnatural fractures caused by the drilling activity and pressure release. Usually, the surface of fractures produced during the drilling activity is uneven, and these fractures do not have obvious directionality. However, the natural fracture surface is relatively flat or even smooth and has a strong directionality. Moreover, because there was no underground fluid flowing through, the surface of fractures produced during the drilling activity and formed by pressure release is very new. Based on these characteristics, we distinguished such unnatural fractures from natural fractures in the observation and statistics of fractures in cores, in order to minimize their influence on the real data.

Natural fractures in borehole image logs usually appear as sinusoidal curves, making it possible to quantify their orientation, dip angle, density, and aperture [47,48]. Moreover, in borehole image logs with water-based mud, opening-mode fractures are usually filled with mud filtrate or low-resistance minerals and appear as dark sinusoidal curves, while filled fractures with high resistance minerals (such as dolomite and calcite) often present as light or white sinusoidal curves [49]. Thin sections with a thickness of 30 μm were made with blue-dye resin to highlight natural fractures and pores, and some of them were impregnated with alizarin red to distinguish calcite and dolomite [50]. These thin sections are divided into two types, vertical and parallel to the wellbore. The specific directions of each thin sections are marked in the captions of Figures. Fractures in these thin sections were observed and measured by the Olycia g3 software from Olympus, Japan [51].

By studying the variation law of the characteristics and intensity of natural fractures, the factors controlling fracture development in these reservoirs were determined. Furthermore, by comparing the lithology, fracture characteristics, and oil production in six perforated intervals, we evaluated the role of natural fractures on oil production and proposed ideas to optimize development plans in the carbonate basement reservoirs to enhance production. It should be noted that, in this analysis, the fracture density refers to the linear density of opening-mode fractures, and oil production refers to the daily production of oil during the well-testing stage.

4. Results

4.1. Fracture Characteristics

This study distinguished three genetic types of natural fractures, including tectonic, pressure-solution, and dissolution fractures, in the basement reservoirs of carbonate rocks in the Jizhong Sub-Basin [39,52,53]. Among these, tectonic fractures have a higher development degree than others and are the dominant type in these reservoirs.

4.1.1. Tectonic Fractures

Tectonic fractures in the outcrops appear in sets, and their occurrences are stable (Figure 4). Statistical analysis of outcrops confirms that tectonic fractures are developed in three major sets of NNE–SSW, NW–SE, and near E–W strikes, while less developed in other directions (Figure 5). On the

cross-section, tectonic fractures may pass through the rock formation interface and have a height of several meters (Figure 4a). Other tectonic fractures within the rock formation with a height of less than a few tens of centimeters were also observed (Figure 4b). On the horizontal plane, tectonic fractures show mutual crosscutting relations, and their lengths vary considerably, from several centimeters to meters (Figure 4c). The dip angles of these fractures are mainly high ($>60^\circ$) and near-horizontal ($<15^\circ$). Ultimately, the number of tectonic fractures with oblique dip angles (15° – 60°) was found less than 20% of the total (1326).

Based on core observations, tectonic fractures usually exhibit a fracture plane with steps (Figure 6a). In mudstones and argillaceous carbonate rocks, these fractures demonstrate clear striae along the direction of fractures propagation, with a very smooth surface (Figure 6b). Borehole image log interpretation indicates that tectonic fractures appear as sinusoidal curves and are randomly distributed (Figure 7a). Some tectonic fractures are intertwined to form a fracture network (Figure 7b). The dip angles of these fractures are concentrated in the range of 60° to 85° , followed by those with angles less than 30° . In particular, the dip angles of fractures in mudstones are mainly less than 20° . The linear density of tectonic fractures in a single well varies notably, ranging from 1.2 m^{-1} to 8.6 m^{-1} . Furthermore, borehole image logs confirm the existence of fracture sets similar to those in the outcrops, mainly in the NNE–SSW, NW–SE, and near E–W strikes. More than 65% of tectonic fractures are opening-mode ones in which minerals are not filled, while others are entirely or partially filled by calcite, hydrocarbons, and clay minerals (Figures 6c and 7c).

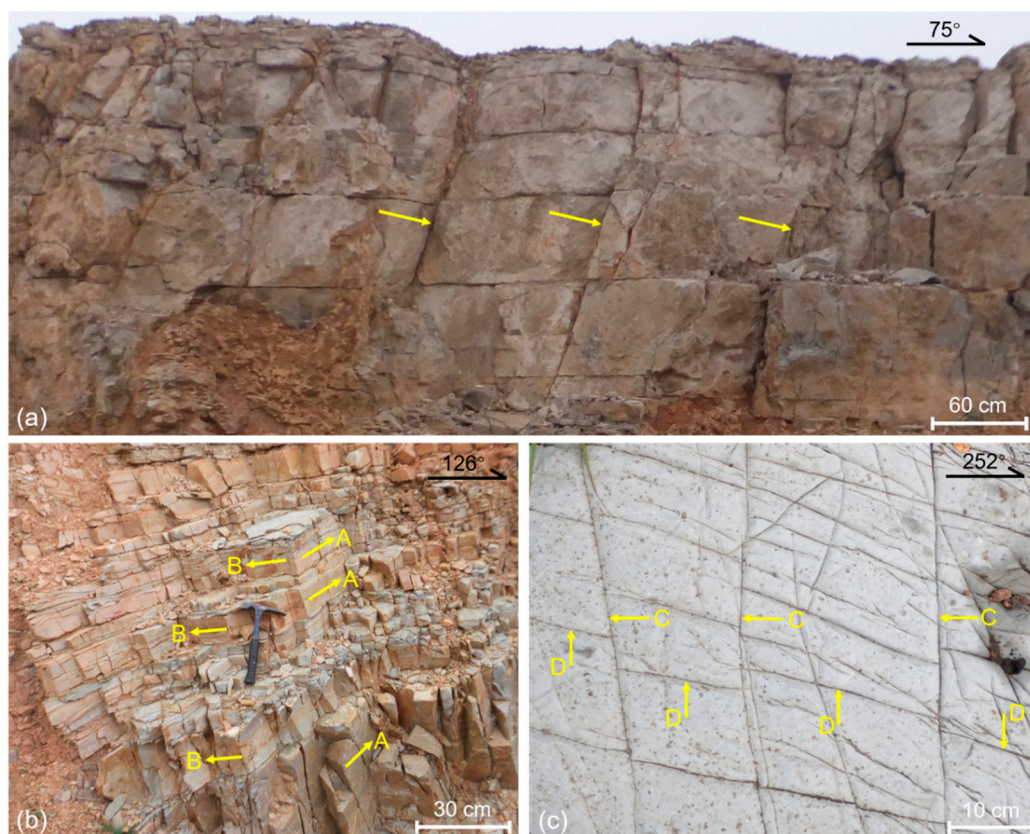


Figure 4. Tectonic fractures in outcrops. (a) Fractures are developed with a height of several meters on the cross-section. (b) Fractures are developed within the rock formation with a height of a few tens of centimeters. (c) Fractures show mutual crosscutting relations on the horizontal plane where Set C arrests Set D.

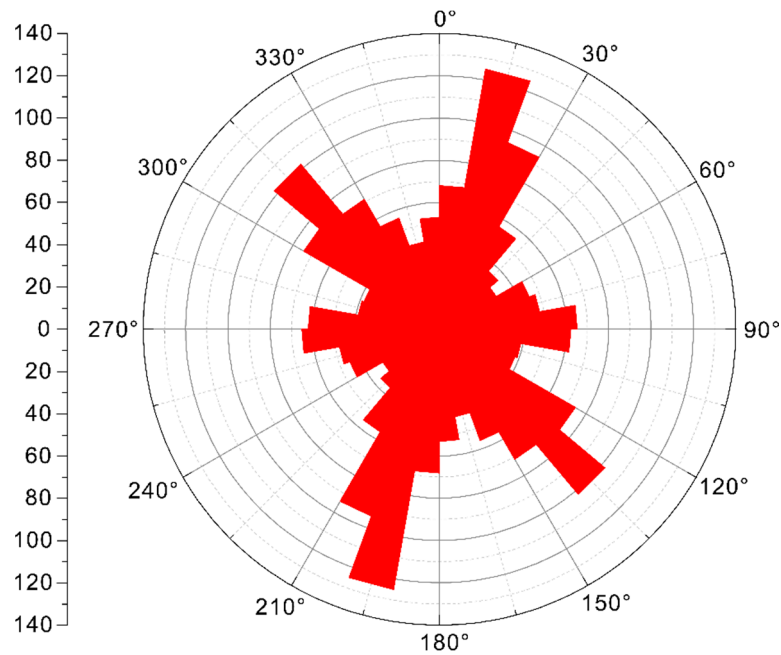


Figure 5. Orientations of tectonic fractures in outcrops of carbonate rocks in the Jizhong Sub-Basin ($n = 1105$).

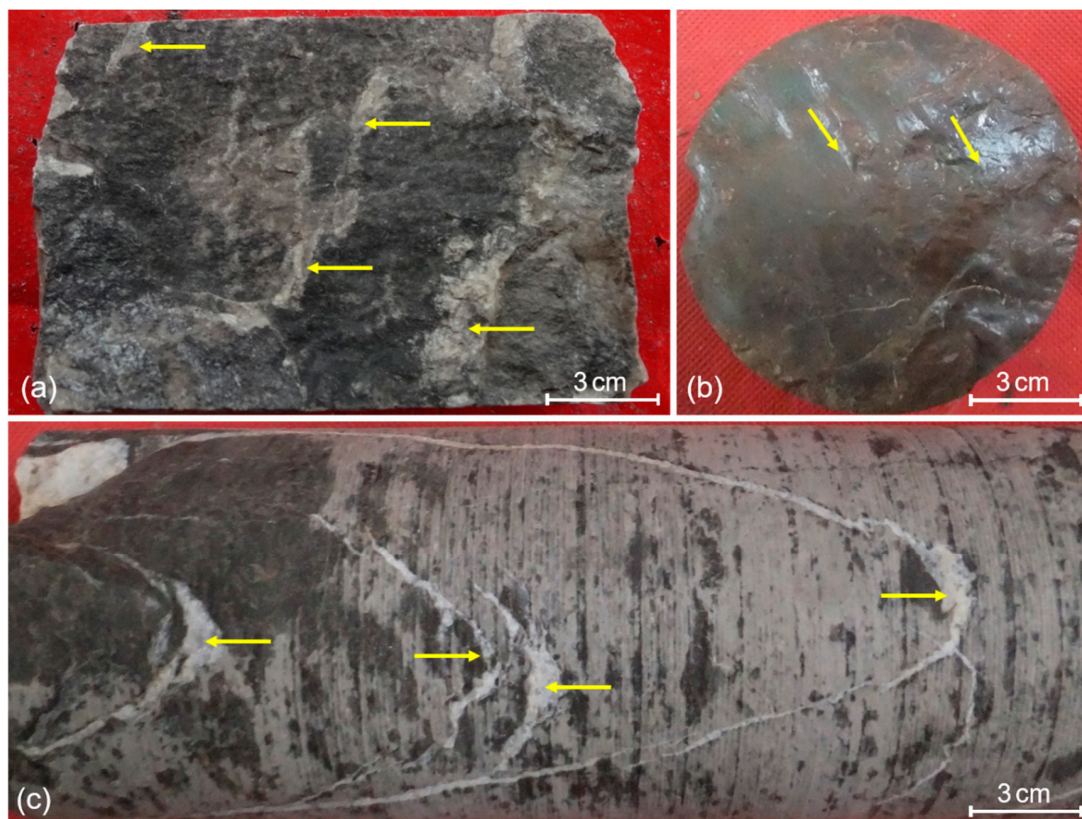


Figure 6. Tectonic fractures in cores. (a) Fractures in Well R6, depth 5583.18 m (18,317.52 ft). (b) Fractures in Well R14, depth 4010.37 m (13,157.38 ft). The dip angle of this fracture is 6° . (c) Fractures in Well R7, depth 4301.19 m (14,111.52 ft). Calcite entirely filled fractures.

The inspection of thin sections reveals that tectonic fractures are widely distributed in these carbonate rocks (Figure 8). Two sets of tectonic fractures can cut through or arrest each other (Figure 8b,c), and multiple sets are interwoven to form a network (Figure 8d). The development of

these fractures does not exhibit any relationship with the bedding plane of carbonate rocks. If early developed fractures are filled with minerals such as calcite, pyrite, clay, or hydrocarbons, they will not provide effective storage space and seepage channels for the reservoir and become ineffective (Figure 8d–f) [54,55]. In this regard, the same fracture could be filled multiple times with different minerals (Figure 8e,f). More than 60% of tectonic fractures in thin sections are open and do not show any mineral fillings. The apertures of these fractures vary, while most of them are less than 100 μm and are concentrated below 60 μm .

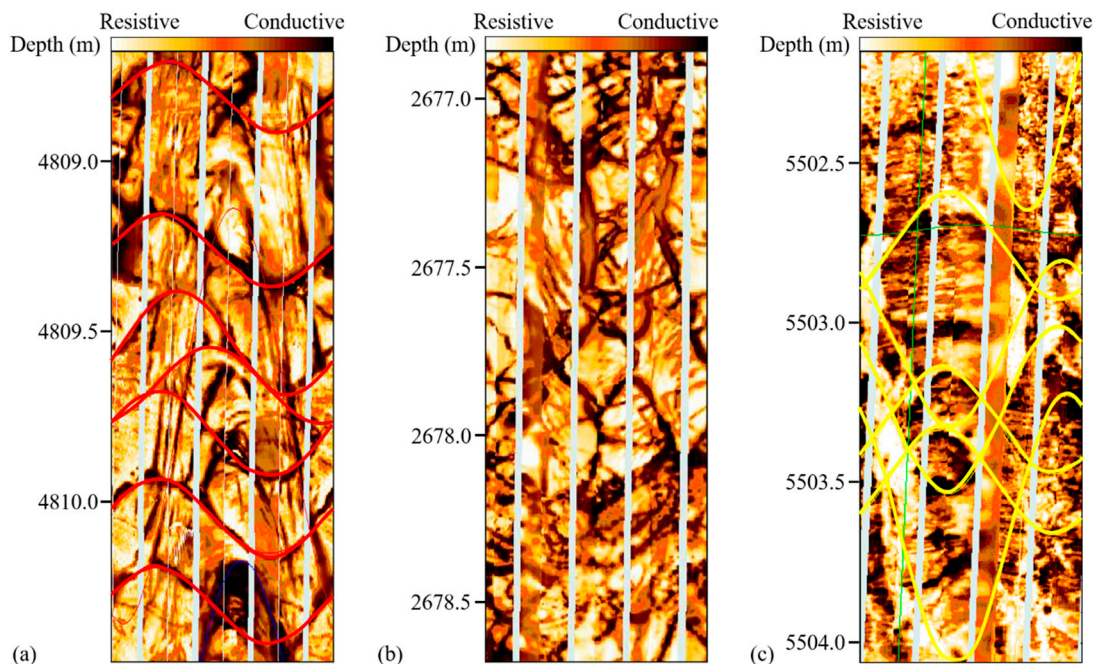


Figure 7. Tectonic fractures in borehole image logs. (a) Tectonic fractures are conductive in Well R8. The red sinusoidal curves represent recognized fractures. (b) Tectonic fractures that are not filled link together like a network in Well R15. (c) Tectonic fractures in Well R3. The yellow sinusoidal curves represent the fractures filled by minerals.

4.1.2. Pressure-Solution Fractures

Pressure-solution fractures are formed during structural and diagenetic processes due to pressure solution [56]. The pressure-solution fractures in these reservoirs are composed of bed-parallel fractures and stylolites. The bed-parallel fractures are formed along the depositional interface under various geological conditions, with distinguishable characteristics such as bending, discontinuity, and branching (Figures 9a–c and 10a) [57]. These fractures exhibit small dip angles and are nearly parallel to the depositional interface. There are normally insoluble mineral residues recognized in them, such as clay minerals, while they can also be filled with hydrocarbons or other minerals. Stylolites are generally irregularly wavy or serrated, parallel or sub-parallel to the horizontal plane, with a small number intersecting the horizontal plane at a small angle (Figures 9c,d and 10b). Iron argillaceous minerals and hydrocarbons can fill some of these fractures. These pressure-solution fractures are poor in lateral continuity, and their apertures in the thin sections are commonly less than 35 μm .

4.1.3. Dissolution Fractures

Dissolution fractures are formed through long-term underground fluid, including the new fracture formed after the dissolution transformed the earlier fracture and the fracture formed when the dissolution connected a lot of pores [58,59]. When dissolution fractures are formed from earlier ones, their fracture walls are rough and uneven, and their apertures are larger than the previous stage fractures (Figure 11a). Although newly dissolved pores are preserved inside or at the edges

of the original fractures and the shape of the initial sets are changed after the dissolution process, the original distribution of these fractures can still be discerned. Dissolution fractures that are formed when multiple pores are connected like a string of beads will become an effective storage space for hydrocarbons in the reservoir (Figure 11b). Besides, fractures filled with minerals can also become dissolution fractures when unstable filling minerals like calcite entirely or partially are dissolved via acidic water leaching or groundwater scouring (Figure 11c,d). Overall, dissolution fractures are irregular in shape, often in the pattern of snake-like and anastomosing (Figures 10c and 11) [60]. The apertures of dissolution fractures measured in thin sections vary significantly and are between 40 μm and 80 μm and sometimes become relatively large (up to 200 μm).

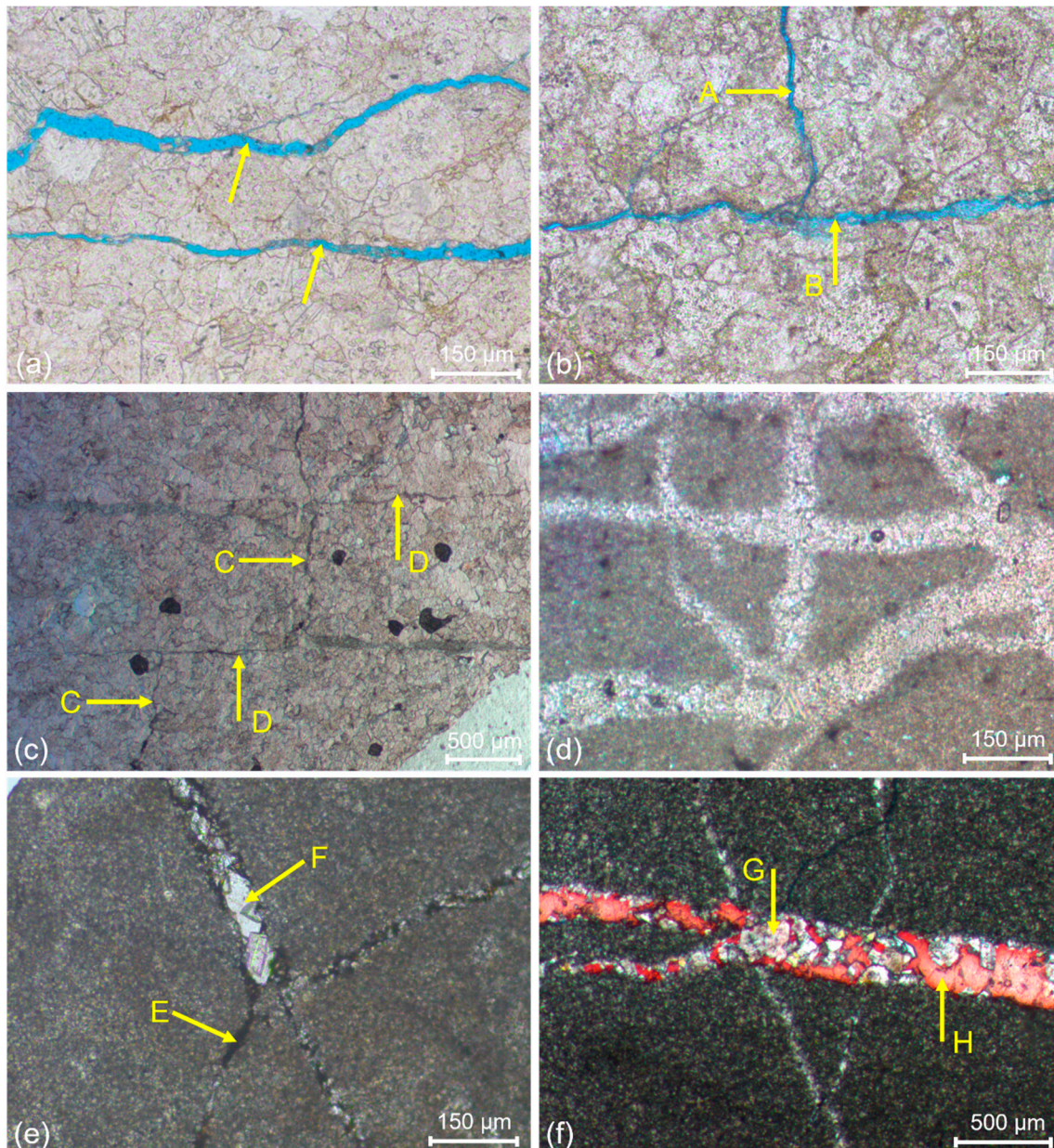


Figure 8. Tectonic fractures in thin sections. (a) Fractures in Well R2, depth 5039.60 m (16,534.12 ft). (b) Fractures in Well R2, depth 5039.35 m (16,533.30 ft). Group B terminated Group A. (c) Fractures in Well R5, depth 5916.02 m (19,409.51 ft). Group D terminated Group C. (d) Fractures are filled with calcite in Well R9, depth 4548.10 m (14,921.59 ft). (e) Fractures in Well R5, depth 5728.31 m (18,793.67 ft). E shows hydrocarbons, and F is calcite. (f) Fractures in Well R8, depth 4703.26 m (15,430.64 ft). G is dolomite, and H is calcite. The directions of these thin sections are vertical to the wellbore.

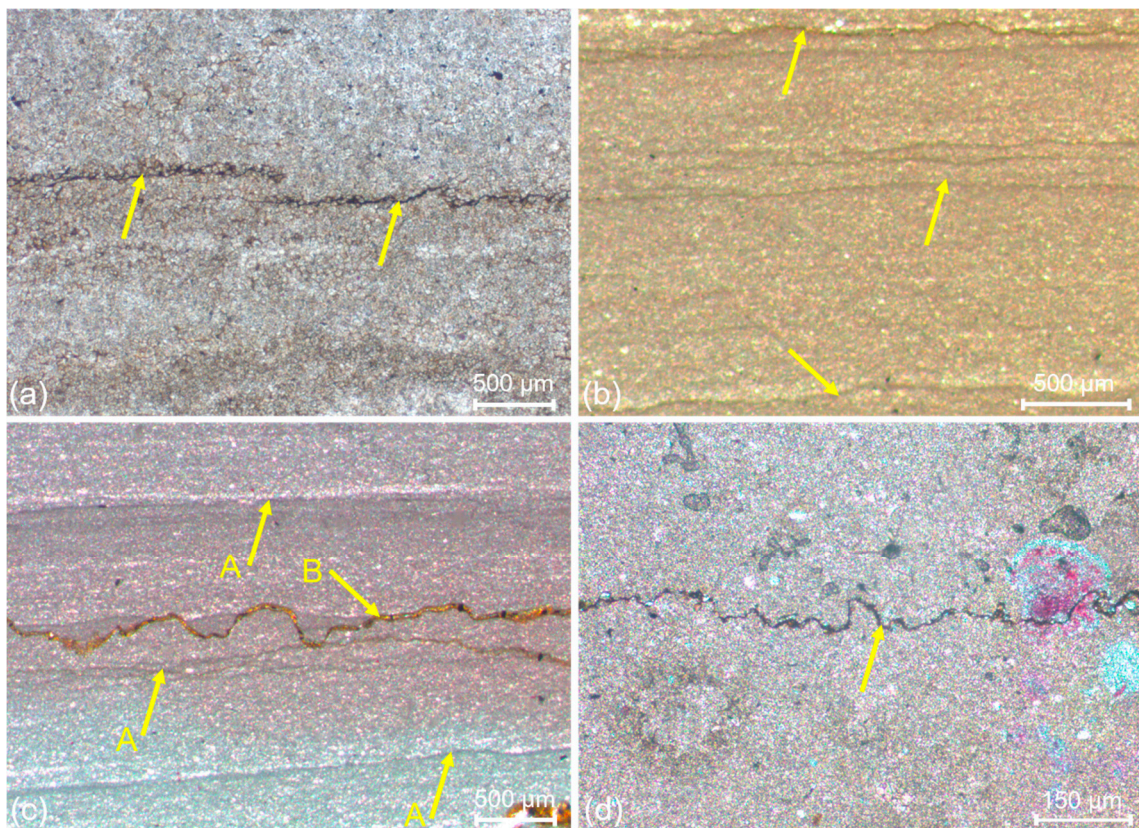


Figure 9. Pressure-solution fractures in thin sections. (a) Bed-parallel fractures in Well R2, depth 5041.27 m (16,539.60 ft). (b) Bed-parallel fractures in Well R8, depth 4861.80 m (15,950.79 ft). (c) Fractures in Well R8, depth 4862.12 m (15,951.84 ft). A is the bed-parallel fracture. B is the stylolite. (d) Stylolite in Well R9, depth 4548.53 m (14,923.00 ft). The directions of these thin sections are parallel to the wellbore.

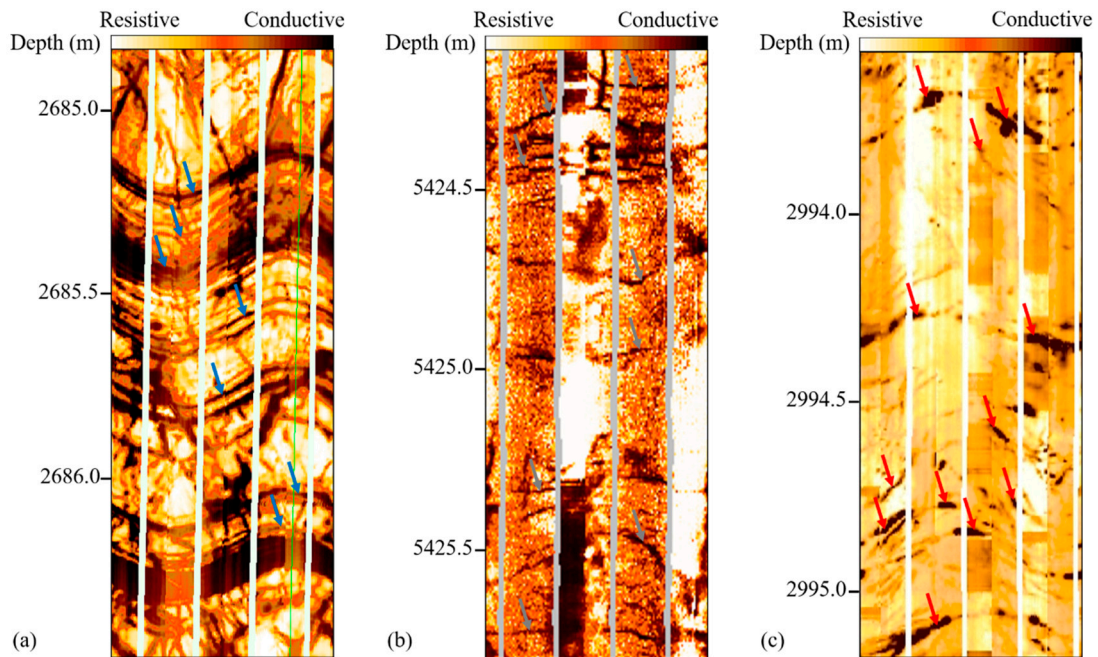


Figure 10. Fractures in borehole image logs. (a) Bed-parallel fractures in Well R15. (b) Stylolites in Well R1. (c) Dissolution fractures in Well R16. The arrows mark the identified fractures.

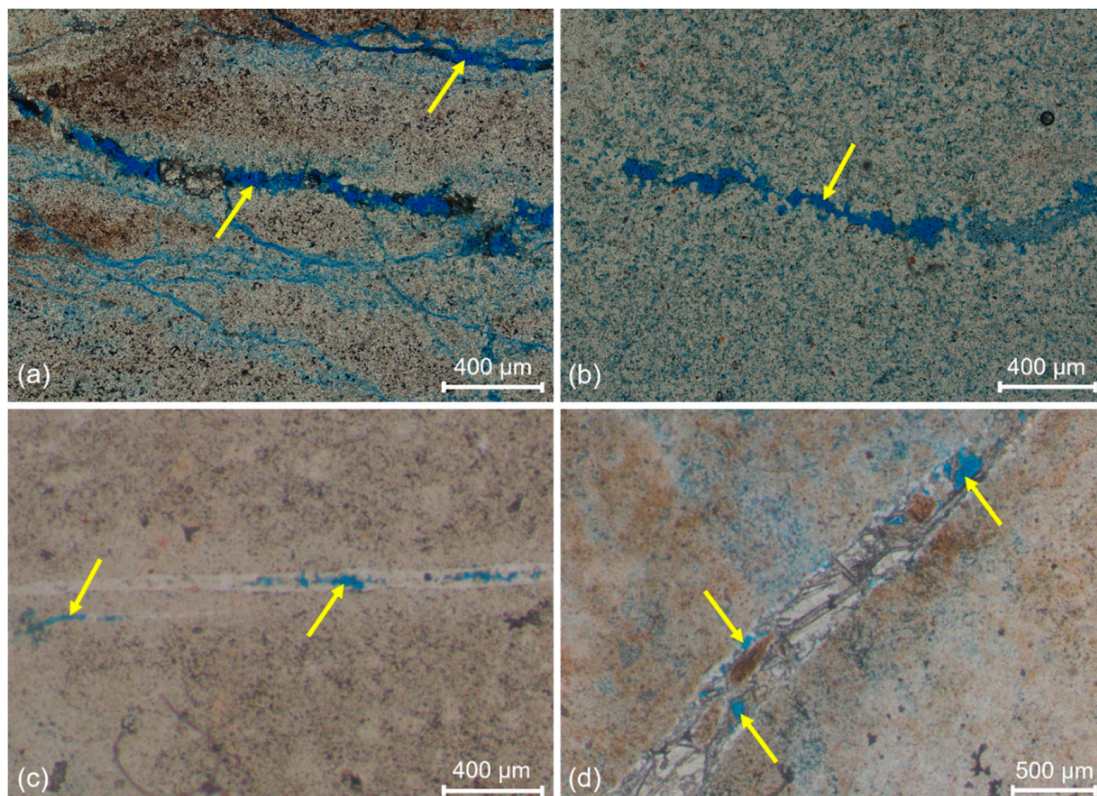


Figure 11. Dissolution fractures in thin sections. (a) Fractures in Well R12, depth 3105.18 m (10,187.60 ft). (b) Fractures in Well R12, depth 3112.35 m (10,211.12 ft). (c) Fractures in Well R17, depth 2764.60 m (9070.21 ft). (d) Fractures in Well R17, depth 2764.00 m (9068.24 ft). The directions of these thin sections are vertical to the wellbore. The minerals dissolved in these filled fractures are calcite.

4.2. Factors Influencing Fracture Development

4.2.1. Lithology

The lithology in the basement reservoirs of carbonate rocks includes dolostone, limestone, and a small amount of mudstone [39]. The development of tectonic fractures is divided into two categories: (1) only one or several sets of tectonic fractures that are developed in the rocks, and they are often regular and can be accurately measured and counted (Figure 7a); and (2) multiple sets of tectonic fractures that are interwoven into a network, which makes it difficult to measure and count each fracture, creating a fracture zone (Figure 7b). Observations and statistical analysis of different lithologies depict that the fracture zone is developed in both dolostone and limestone, but barely in mudstone (Figure 12). Based on borehole image logs, the ratio of the fracture zone thickness to the rock thickness in dolostone is 18.1%, while in limestone, it is 12.5%. Moreover, the linear density of tectonic fractures in the borehole image logs, excluding the fracture zone, was also analyzed (Figure 12). Hereof, the average linear density of tectonic fractures in dolostone is found the largest, which can reach 6.8 m^{-1} , followed by limestone, and finally mudstone, 4.1 m^{-1} and 1.3 m^{-1} , respectively. Also, in the outcrops, tectonic fractures are more developed in dolostone than limestone, while tectonic fractures in mudstone have the least development degree (Figure 13). All of these indicate that lithology controls the abundance of tectonic fractures in the target layers.

Lithology controlling fracture development is essentially due to the rock composition, particle size, and particle arrangement [61,62]. Both dolomite and calcite are the major minerals in carbonate rocks, but the Young's modulus of dolomite (8.71×10^4 – 14.18×10^4 MPa) is higher than calcite (5.69×10^4 – 8.82×10^4 MPa) [63–65]. Therefore, under the same stress conditions, dolostone with higher dolomite content is more likely to develop tectonic fractures than limestone with higher calcite content. However,

the abundance of these minerals (calcite and dolomite) in the mudstone is very low, hence tectonic fractures are developed poorly. Based on thin sections, limestone is more likely to host dissolution fractures than dolostone and mudstone due to its higher calcite content [66].

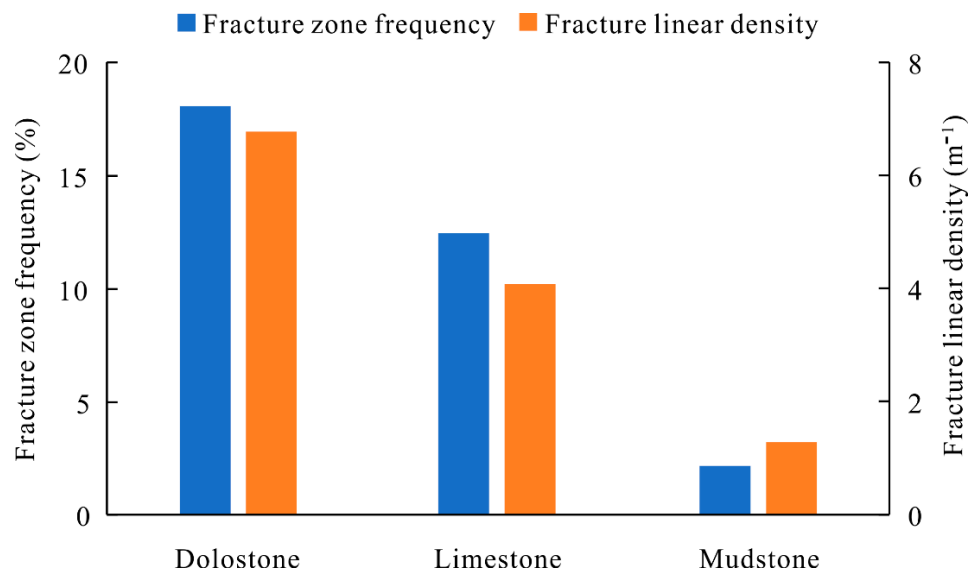


Figure 12. Schematic diagram comparing the fracture zone frequency and fracture linear densities of tectonic fractures in different lithologies. The fracture zone frequency refers to the ratio of the fracture zone thickness to the rock thickness based on borehole image logs.



Figure 13. Tectonic fractures in different lithologies of carbonate rocks in the outcrops.

4.2.2. Mechanical Stratigraphy

Mechanical stratigraphy subdivides stratified rock into discrete mechanical units consisting of one or more stratified rock units with consistent or similar rock mechanical properties such as brittleness, tensile strength, elastic stiffness, and fracture mechanics properties [49,67,68]. These mechanical units are generally, but not always, one layer with uniform lithology, which is not exactly the same as the lithologic layer. Further analysis in these basements reveals that mechanical stratigraphy which controls tectonic fractures can work in two ways: (1) the interface of the mechanical unit controls the

growth and termination of tectonic fractures, and (2) the thickness of the mechanical unit controls the development degree and height of tectonic fractures.

Tectonic fractures in the outcrops mainly are developed inside the mechanical unit, and most of them cut through the entire mechanical unit and end at the interface of two separate mechanical units (Figure 14). These fractures are nearly perpendicular to or are inclined at a high angle to the interface of mechanical units. As the mechanical unit thickness increases, the height of tectonic fractures increases as well. Based on core observations, tectonic fractures only are developed in the same mechanical unit and terminated at the interface when lithological variations dictate a different mechanical unit (Figure 15). Moreover, tectonic fractures of the same set are developed at approximately equal intervals in the same mechanical unit. The outcrop observations show that in the mechanical units that are limited in thickness, the mean spacing of tectonic fractures displays a strong linear relationship with the thickness of mechanical units, which means the mean spacing of tectonic fractures increases as the thickness of mechanical units increases (Figure 16) [45,69,70]. Consequently, the stress regime has caused tectonic fractures in the thinner mechanical unit to be more frequent and with smaller heights, unlike thicker mechanical units.



Figure 14. The outcrop section shows tectonic fractures in different mechanical units. I to V refer to the number of mechanical units. The linear density of tectonic fractures is 4.3 m^{-1} in I, 10.6 m^{-1} in II, 9.3 m^{-1} in III, 3.6 m^{-1} in IV, and 6.7 m^{-1} in V.

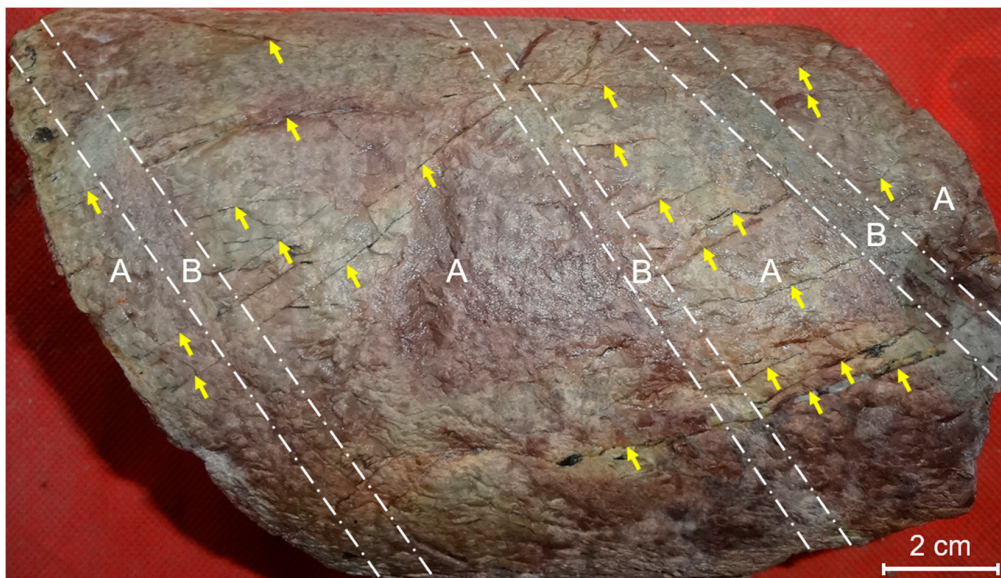


Figure 15. Tectonic fractures in the cores of Well R15, depth 2598.08 m (8523.88 ft). The fractures are mainly developed in layer A and end at the interface between separate layers A and B.

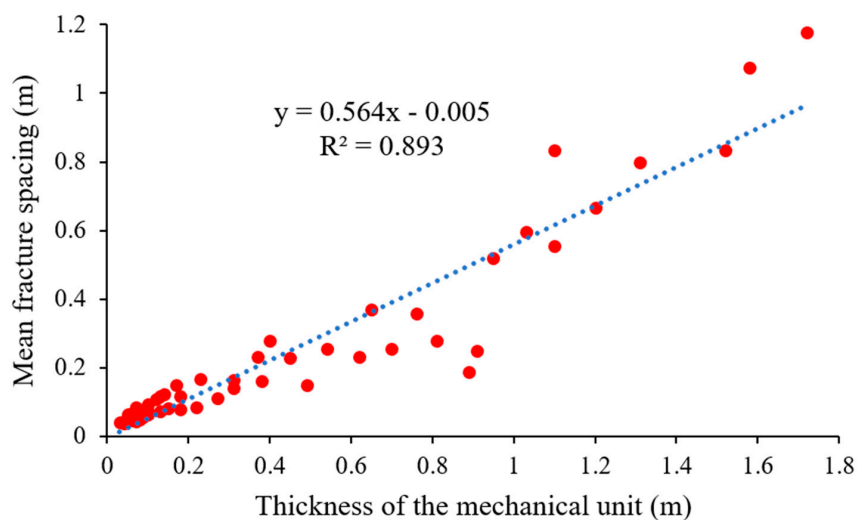


Figure 16. The relationship between the mean fracture spacing and the thickness of mechanical units from 52 data points on outcrops.

4.2.3. Fault

Since the Paleozoic, the Jizhong Sub-basin has experienced three large-scale tectonic movements: Indosinian, Yanshan, and Himalayan movements, to form a typical multi-period structural superimposed sub-basin [39]. The sub-basin mainly has caused two-set extensional fault systems of NNE-SSW and NW-SE strikes, in addition to some near E-W strikes [34,42] (Figure 17). The characteristics of these faults indicate that the faults with NNE-SSW strikes are major ones that control the orientations of deep tectonic belts, and the faults with NW-SE and near E-W strikes are the lateral faults which segment the tectonic belts and control the formation and scale of deep reservoirs [44]. Interpretations of borehole image logs explain that tectonic fractures in these reservoirs are mainly NNE-SSW, NW-SE, and near E-W strikes overall. Nevertheless, in different locations of the sub-basin, fracture directions vary notably (Figure 17). In the northeastern and southwestern regions of this sub-basin, the dominant direction of tectonic fractures is the NNE-SSW strikes, while in the central part and near the transfer zones, the dominant direction of these tectonic fractures becomes more complicated where all the three sets (NNE-SSW, NW-SE and near E-W strikes) can appear.

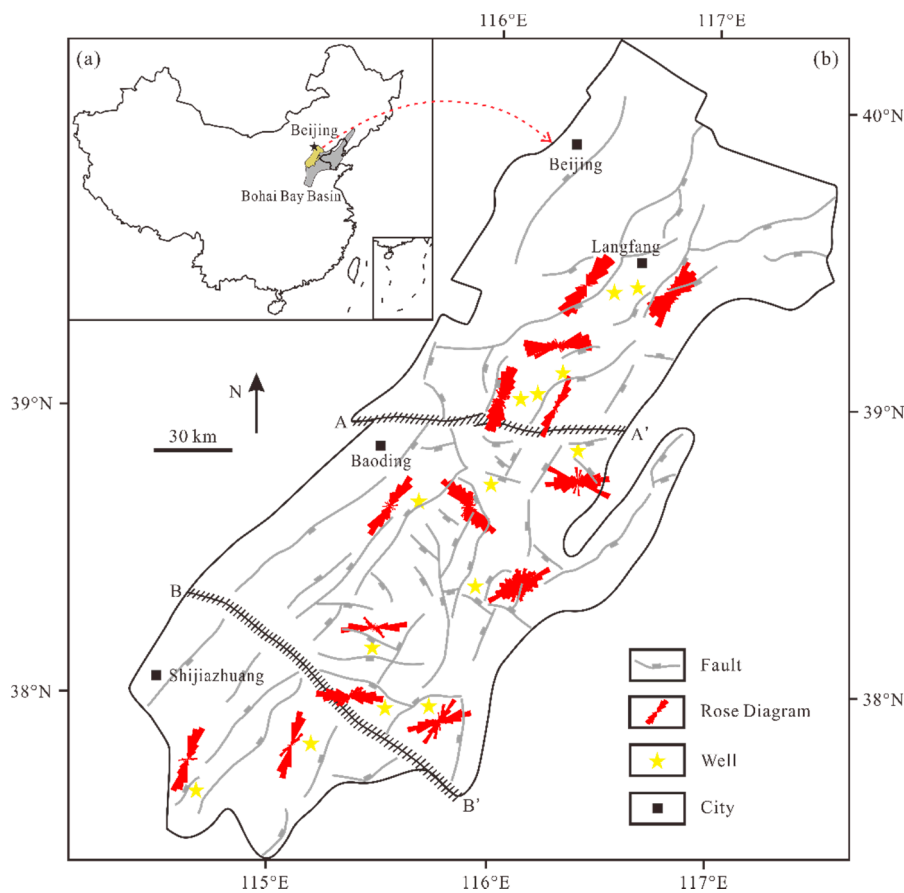


Figure 17. The relationship between fault and fracture strikes. (a) Location of the Jizhong Sub-Basin in the Bohai Bay Basin in China (modified from Zhao et al., 2015) [9]. (b) Faults and tectonic fracture orientations in the carbonate rocks of the Jizhong Sub-basin. The fault data was modified from the Huabei Oilfield database. The data regarding fracture orientations is derived from the borehole image logs of 14 wells.

The main reason is that the NNE–SSW strike faults are the only one set that is developed in the northeastern and southwestern regions of this sub-basin and all the NNE–SSW, NW–SE, and near E–W strike faults are developed in the central area of the sub-basin. The orientation of the fractures and faults is consistent, and the dominant direction of these fractures is sub-parallel to the direction of faults or oblique at a smaller angle. Therefore, one can conclude that tectonic fractures in this sub-basin are associated with faults, and these faults have a significant influence on the fracture direction.

5. Discussion

The basement reservoirs of carbonate rocks that are discovered in the Jizhong Sub-Basin in the Bohai Bay Basin are mainly dolostones and limestones from the Mesoproterozoic, Neoproterozoic, and Lower Paleozoic periods [38]. Reservoir properties determine the oil and gas accumulation in these reservoirs [17,71,72]. Initial structures and pores of carbonate rocks in these basements are mostly transformed by recrystallization, dolomitization, and tectonism, and has formed the interconnected composite reservoir system consisting of pores and fractures [18,19]. Qiao et al. (2002) studied the relationship between the porosity and burial depth of 32 carbonate basement reservoirs in the Bohai Bay Basin [73]. They found that the porosity does not decrease significantly with the increase of burial depth, while the average porosity generally varies between 5% and 6%, with a negligible change. This infers that because the height variation is not significant in these reservoirs, pores are less affected by the buried depth, and a relatively larger amount of porosity can stay intact to provide a suitable reservoir quality [71]. Moreover, a single basement reservoir has a relatively uniform pressure system and small

changes in fluid properties, and the lithology distribution in the reservoir is relatively stable [9,18,19,38]. However, the above research results show that the development of fractures in these reservoirs has strong heterogeneity. Observations from outcrops, cores, borehole image logs, and thin sections show that these fractures are usually connected (Figures 4 and 6–8). We speculate that the development of opening-mode fractures improves the effectiveness of the storage space, thereby influencing the reservoir's effective permeability and oil production in these carbonate basement reservoirs.

Through a comprehensive analysis of lithology, opening-mode fractures, and well-testing data, we found that geological characteristics and oil production in the carbonate basement reservoirs vary regionally within the reservoir unit. Considering Well R10, which is drilled in a typical basement inner reservoir with a total of 6 perforated intervals at a depth of 4095–4142 m (13,435.0–13,589.2 ft), significant differences in oil production from each perforated interval is reported (Figure 18). Among them, the V and VI perforated intervals displayed higher oil production, 16.62 and 45.58 tons per day (124.30 barrels and 340.95 barrels per day), respectively, making them the main oil production section of Well R10. These intervals are followed by the II and III perforated intervals, with oil production of 4.94 tons and 6.53 tons per day (36.93 barrels and 48.88 barrels per day), respectively. Finally, perforated intervals I and IV are dry layers without any oil production. The lithologic comparison of different perforated intervals indicates that the I and IV perforated intervals without any oil production are mainly limestones, especially the I perforated interval, which is only limestones. In this regard, other perforated intervals with oil production have different degrees of dolostone content where in the V and VI perforated intervals with the largest quantities of oil production, dolostone and limestone are interstratified (Figure 18).

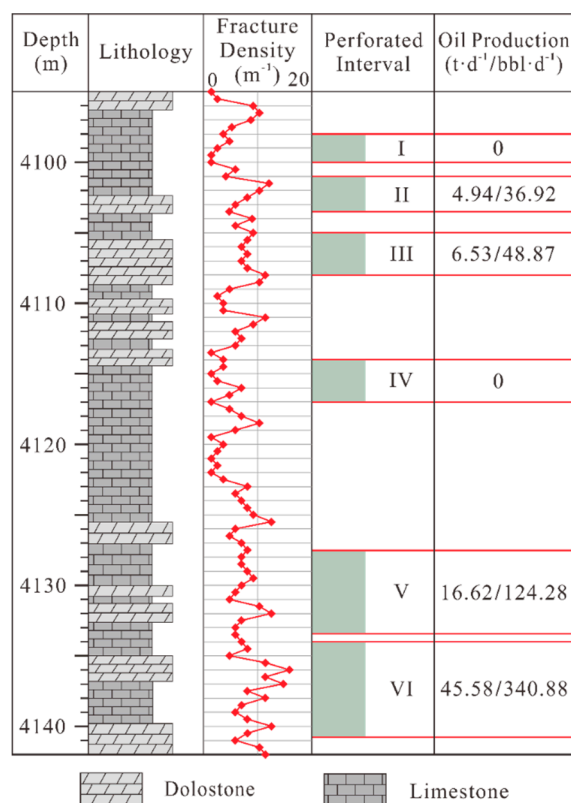


Figure 18. Schematic diagram showing the lithology combination, fracture density, perforated interval, and oil production in Well R10. Oil production refers to the daily production of oil in the well-testing stage. Lithology and fracture data were derived from the borehole image logs, and the data pertaining to perforated intervals and oil production were collected from the Huabei Oilfield database. I to VI refer to the name of perforated intervals, which correspond to the names also shown separately in Figure 19. Unit t·d⁻¹ refers to the average number of tons of oil produced per day.

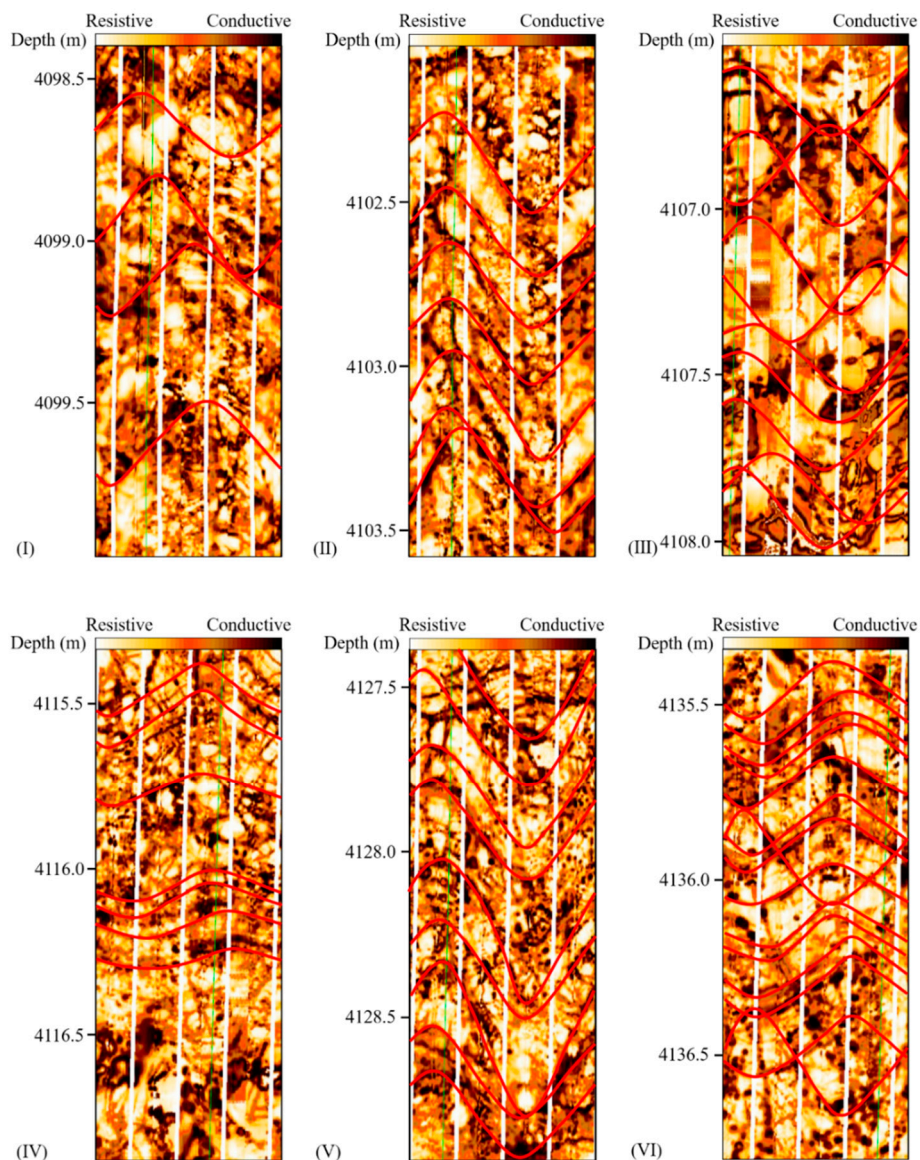


Figure 19. Tectonic fractures in the borehole image logs from Well R10. I to VI represent a part of each perforated interval, respectively. Perforated interval numbers are similar to Figure 18. Red lines represent tectonic fractures that appear as sinusoidal curves.

Fracture interpretations from borehole image logs reveal that opening-mode fractures are well developed at a depth of 4095 m to 4142 m (13,435.0 ft to 13,589.2 ft) in the Well R10, and the average fracture linear density can reach 6.78 m^{-1} . Besides, the development degree and dip angle of these fractures in different perforated intervals demonstrate a large discrepancy (Figure 19). In this aspect, comparing the oil production with the fracture linear density of each perforated intervals, a positive correlation can be found, which means higher fracture linear density can lead to better oil production (Figures 18 and 19). Considering II, III, V, and VI perforated intervals with higher oil production, opening-mode fractures are developed better, and their dip angles are usually greater than 45° (Figure 19II–VI). However, opening-mode fractures are developed less in the I and IV perforated intervals where layers are dry (Figure 19I,IV). In particular, the dip angles of these fractures in IV perforated interval are lower than 45° , and some are even near horizontal.

Geological characteristics of these perforated intervals reveal that the primary reason for different oil production is the varying degree of regional development of opening-mode fractures. Specifically, oil production grows with the increasing of fractures density (Figure 20). In the intervals where the

dolostone and limestone are interstratified or dolostone makes up the primary lithology, fractures are generally more developed, thus the oil production is higher. However, in the intervals with higher quantities of limestone, the development of opening-mode fractures is relatively poor, and the oil production is lower as well. In addition, tectonic fractures are the dominant type of natural fractures in these basement reservoirs, and their effectiveness varies with the dip angles where tectonic fractures with smaller dip angles exhibit smaller aperture because of the overburden stress. This has caused their connectivity to become relatively poor, thus, their contribution becomes less to oil production [50,74,75]. Also, when the dip angle of tectonic fractures becomes larger, aperture increases and their contribution to oil production enhances. Therefore, it is deduced that tectonic fractures play a major role in the quality of basement reservoirs with carbonate rocks in the Jizhong Sub-basin, and their development has a significant impact on the oil production from these reservoirs.

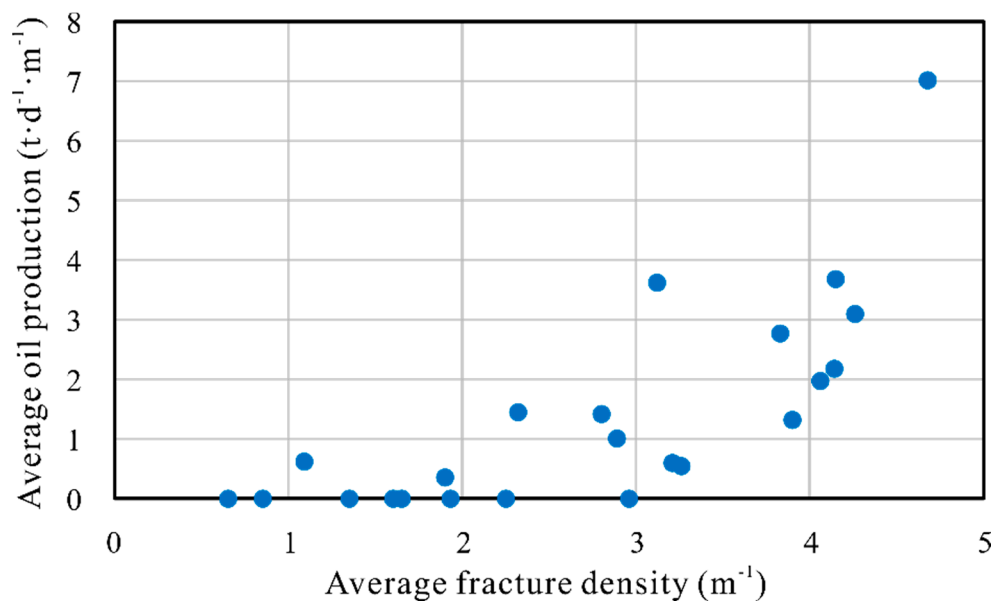


Figure 20. The relationship between the average oil production and the average fractures density in the perforated intervals. The average oil production refers to the daily production of oil in the well-testing stage in every meter perforated interval. The average fracture density is the linear density of opening-mode fractures in the perforated interval from the borehole image logs. Unit $t \cdot d^{-1} \cdot m^{-1}$ refers to the average number of tons of oil produced per day in one-meter perforated interval.

6. Conclusions

This study indicates that natural fractures are abundant in genetic types, including tectonic, pressure-solution, and dissolution ones, in the carbonate basement reservoirs in the Jizhong Sub-Basin, where tectonic fractures are the dominant type. Macroscopic fractures vary in height and length from several centimeters to meters, with a wide range of linear densities and dip angles. These fractures are found in three sets of NNE–SSW, NW–SE, and near E–W strikes. The apertures of microscopic fractures are concentrated below 60 μm , and more than 60% of them are opening-mode ones without mineral fillings.

Dolostones with higher dolomite content are more likely to develop tectonic fractures than limestones with higher calcite content, and tectonic fractures have the least development intensity in the mudstone. Most tectonic fractures are developed inside the mechanical units and end almost perpendicularly or with a higher angle to the mechanical unit interface. In a thinner mechanical unit, these fractures are more frequent and have a smaller height. The dominant orientation of fractures changes regularly and is sub-parallel to faults or oblique at a small angle.

The analysis of opening-mode fractures and well-testing data in perforated intervals reveals that oil production is related to fracture characteristics. In intervals where dolostone and limestone are

interstratified or dolostone is the main lithologic composition, fractures are generally more developed, and oil production is higher, unlike intervals where limestone is the main constituent. Moreover, tectonic fractures with larger dip angles present a bigger aperture and contribute more to oil production. Finally, it is concluded that natural fractures are the main controlling factor of oil production to create favorable reservoir conditions in these basements. This study provides reference and future guidance for a better understanding of natural fractures and reservoir heterogeneity in the basement reservoirs of carbonate rocks.

Author Contributions: Conceptualization, G.L. and L.Z.; Data curation, C.H. and F.H.; Formal analysis, G.L.; Investigation, W.L. and J.Z.; Resources, C.H. and F.H.; Software, J.Z.; Supervision, L.Z.; Validation, W.L. and J.Z.; Writing—original draft, G.L.; Writing—review and editing, L.Z., M.O. and Q.W. All authors have read and agreed to the published version of the manuscript.

Funding: This research was funded by the National Major Science and Technology Projects of China, grant number 2017ZX05008-006-002-005.

Acknowledgments: The authors greatly acknowledge the Petro China Huabei Oilfield Company for providing information and other support. The authors would also like to thank the work made by Li Jian and Lyu Peng in the China University of Petroleum-Beijing, which enabled our study to proceed successfully. We are also particularly grateful to Veljko Pajovic and three anonymous reviewers for providing constructive comments and suggestions, which improve our manuscript significantly.

Conflicts of Interest: The authors declare no conflict of interest.

References

1. P'an, C.H. Petroleum in basement rocks. *AAPG Bull.* **1982**, *66*, 1597–1643.
2. Petford, N.; McCaffery, K.J.W. Hydrocarbons in Crystalline Rocks: An introduction. *Geol. Soc. Lond. Spec. Publ.* **2003**, *214*, 1–5. [[CrossRef](#)]
3. Sircar, A. Hydrocarbon production from fractured basement formations. *Curr. Sci.* **2004**, *87*, 147–151.
4. Luo, J.; Morad, S.; Liang, Z.; Zhu, Y. Controls on the quality of Archean metamorphic and Jurassic volcanic reservoir rocks from the Xinglongtai buried hill, western depression of Liaohe basin, China. *AAPG Bull.* **2005**, *89*, 1319–1346. [[CrossRef](#)]
5. Price, L.C. Thermal stability of hydrocarbons in nature: Limits, evidence, characteristics, and possible controls. *Geochem. Cosmochem. Acta* **1993**, *57*, 3261–3280. [[CrossRef](#)]
6. Gao, X.; Pang, X.; Li, X.; Chen, Z.; Shan, J.; Liu, F.; Zou, Z.; Li, W. Complex petroleum accumulating process and accumulation series in the buried-hill trend in the rift basin: An example of Xinglongtai structure trend, Liaohe subbasin. *Sci. China Ser. D Earth Sci.* **2008**, *51*, 108–116. [[CrossRef](#)]
7. Jin, Q.; Zhao, X.; Jin, F.; Ma, P.; Wang, Q.; Wang, J. Generation and accumulation of hydrocarbons in a deep “buried hill” structure in the baxian depression, bohai bay basin, eastern China. *J. Pet. Geol.* **2014**, *37*, 391–404.
8. Schubert, F.; Diamond, L.W.; Tóth, T.M. Fluid-inclusion evidence of petroleum migration through a buried metamorphic dome in the Pannonian Basin, Hungary. *Chem. Geol.* **2007**, *244*, 357–381. [[CrossRef](#)]
9. Zhao, X.; Jin, F.; Wang, Q.; Bai, G. Buried-hill play, Jizhong subbasin, Bohai Bay basin: A review and future prospectivity. *AAPG Bull.* **2015**, *99*, 1–26. [[CrossRef](#)]
10. Wang, Q.; Laubach, S.E.; Gale, J.; Ramos, M.J. Quantified fracture (joint) clustering in Archean basement, Wyoming: Application of Normalized Correlation Count method. *Pet. Geosci.* **2019**, *25*, 415–428. [[CrossRef](#)]
11. Trice, R. Basement exploration, West of Shetlands: Progress in opening a new play on the UKCS. *Geol. Soc. Lond. Spec. Publ.* **2014**, *397*, 81–105. [[CrossRef](#)]
12. Parnell, J.; Baba, M.; Bowden, S.; Muirhead, D. Subsurface biodegradation of crude oil in a fractured basement reservoir, Shropshire, UK. *J. Geol. Soc.* **2017**, *174*, 655–666. [[CrossRef](#)]
13. Cuong, T.X.; Warren, J.K. Bach Ho field, a fractured granitic basement reservoir, Cuu Long basin, offshore Se Vietnam: A “Buried-hill” play. *J. Pet. Geol.* **2009**, *32*, 129–156. [[CrossRef](#)]
14. Jin, Q.; Mao, J.; Du, Y.; Huang, X. Fracture filling mechanisms in the carbonate buried-hill of Futai Oilfield in Bohai Bay Basin, East China. *Pet. Explor. Dev.* **2015**, *42*, 497–506. [[CrossRef](#)]
15. Zang, M.; Wu, K.; Cui, Y.; Du, W. Types of buried hill and its hydrocarbon accumulation in Jizhong Depression. *J. Oil Gas Technol.* **2009**, *31*, 166–169.

16. Deng, J.; Shi, H.; Wang, B.; Wang, G.; Chen, G. Characteristics and main controlling factors of Paleozoic carbonate buried-hill gas reservoirs in Bozhong Sag. *Pet. Geol. Oilfield Dev. Daqing* **2015**, *34*, 15–20.
17. Kosa, E.; Hunt, D.W. Heterogeneity in Fill and Properties of Karst-Modified Syndepositional Faults and Fractures: Upper Permian Capitan Platform, New Mexico, U.S.A. *J. Sediment. Res.* **2006**, *76*, 131–151. [[CrossRef](#)]
18. Wang, J.; Zhao, L.; Zhang, X.; Yang, Z.; Cao, H.; Chen, L.; Shan, F.; Liu, M. Buried hill karst reservoirs and their controls on productivity. *Pet. Explor. Dev.* **2015**, *42*, 852–860. [[CrossRef](#)]
19. Liu, N.; Qiu, N.; Chang, J.; Shen, F.; Wu, H. Hydrocarbon migration and accumulation of the Suqiao buried-hill zone in Wen'an Slope, Jizhong Subbasin, Bohai Bay Basin, China. *Mar. Pet. Geol.* **2017**, *86*, 512–525. [[CrossRef](#)]
20. Eig, K.; Bergh, S.G. Late Cretaceous-Cenozoic fracturing in Lofoten, North Norway: Tectonic significance, fracture mechanisms and controlling factors. *Tectonophysics* **2011**, *499*, 190–205. [[CrossRef](#)]
21. Joudaki, M.; Farzipour-Saein, A.; Nilfouroushan, F. Kinematics and surface fracture pattern of the Anaran basement fault zone in NW of the Zagros fold-thrust belt. *Int. J. Earth. Sci.* **2016**, *105*, 869–883. [[CrossRef](#)]
22. Gong, L.; Fu, X.; Gao, S.; Zhao, P.; Luo, Q.; Zeng, L.; Yue, W.; Zhang, B.; Liu, B. Characterization and prediction of complex natural fractures in the tight conglomerate reservoirs: A fractal method. *Energies* **2018**, *11*, 2311. [[CrossRef](#)]
23. Loza Espejel, R.; Alves, T.M.; Blenkinsop, T.G. Distribution and growth styles of isolated carbonate platforms as a function of fault propagation. *Mar. Pet. Geol.* **2019**, *107*, 484–507. [[CrossRef](#)]
24. Ding, W.; Zhu, D.; Cai, J.; Gong, M.; Chen, F. Analysis of the developmental characteristics and major regulating factors of fractures in marine-continental transitional shale-gas reservoirs: A case study of the Carboniferous-Permian strata in the southeastern Ordos Basin, central China. *Mar. Pet. Geol.* **2013**, *45*, 121–133. [[CrossRef](#)]
25. Nabawy, B.S. Estimating porosity and permeability using Digital Image Analysis (DIA) technique for highly porous sandstones. *Arab. J. Geosci.* **2014**, *7*, 889–898. [[CrossRef](#)]
26. Guo, P.; Lei, L.; Ren, D. Simulation of three-dimensional tectonic stress fields and quantitative prediction of tectonic fracture within the Damintun Depression, Liaohe Basin, northeast China. *J. Struct. Geol.* **2016**, *86*, 211–223. [[CrossRef](#)]
27. Milad, B.; Slatt, R. Impact of lithofacies variations and structural changes on natural fracture distributions. *Interpretation* **2018**, *6*, T873–T887. [[CrossRef](#)]
28. Milad, B.; Ghosh, S.; Slatt, R.; Marfurt, K.; Fahes, M. Practical aspects of upscaling geocellular geological models for reservoir fluid flow simulations: A case study in integrating geology, geophysics, and petroleum engineering multiscale data from the Hunton Group. *Energies* **2020**, *13*, 1604. [[CrossRef](#)]
29. Gao, C.; Zhang, X.; Zha, M.; Wang, X. Characteristics of buried hill reservoir in Jizhong Depression. *Lithol. Reserv.* **2011**, *23*, 6–12.
30. Ju, W.; Wu, C.F.; Wang, K.; Sun, W.F.; Li, C.; Chang, X.X. Prediction of tectonic fractures in low permeability sandstone reservoirs: A case study of the Es-3(m) reservoir in the Block Shishen 100 and adjacent regions, Dongying Depression. *J. Pet. Sci. Eng.* **2017**, *156*, 884–895. [[CrossRef](#)]
31. Zhao, L.; Jiang, Y.; Liu, H.; Fan, B. Thermal evolution of Paleogene source rocks and relationship with reservoir distribution in Raoyang Sag, Bohai Bay Basin. *Pet. Geol. Recover. Effic.* **2012**, *19*, 1–4.
32. Wu, X.; Niu, J.; Wu, F.; Liu, X. Major control factors of hydrocarbon accumulation in Ordovician interior buried hills, Bohaiwan Basin. *Mar. Orig. Pet. Geol.* **2013**, *18*, 1–12.
33. Yang, M.; Liu, C.; Yang, B.; Zhao, H. Extensional structures of the Paleogene in the central Hebei Basin, China. *Geol. Rev.* **2002**, *48*, 58–67.
34. Su, L.; Luo, P.; Zou, H.; Shi, B.; Zheng, X. Hydrocarbon accumulation conditions of the Ordovician buried hills in the slope zone of the Jizhong Depression. *Geotecton. Metallog.* **2003**, *27*, 191–196.
35. Chang, J.; Qiu, N.; Zhao, X.; Xu, W.; Xu, Q.; Jin, F.; Han, C.; Ma, X.; Dong, X.; Liang, X. Present-day geothermal regime of the Jizhong Depression in Bohai Bay Basin, East China. *Chin. J. Geophys.* **2016**, *59*, 1003–1016.
36. He, D.F.; Cui, Y.Q.; Zhang, Y.Y.; Shan, S.Q.; Xiao, Y.; Zhang, C.B.; Zhou, C.A.; Gao, Y. Structural genetic types of paleoburied hill in Jizhong depression, Bohai Bay Basin. *Acta Petrol. Sin.* **2017**, *33*, 1338–1356.
37. Wu, X.; Lv, Y.; Tian, J.; Guo, Y. Characteristics and evaluation of carbonate buried hill inner cap rock in Jizhong Depression. *Lithol. Reserv.* **2011**, *23*, 49–54.

38. Zhang, W.; Yang, D.; Chen, Y.; Qian, Z.; Zhang, C.; Liu, H. Sedimentary Structural Characteristics and Hydrocarbon Distributed Rules of Jizhong Depression. *Acta Geol. Sin.* **2008**, *82*, 1103–1112.
39. Xiao, Y.; Liu, G.; Han, C.; Zhu, J.; Zhou, C.; Lv, W.; Gao, Y.; Zeng, L.; Ma, X. Development characteristics and main controlling factors of natural fractures in deep carbonate reservoirs in the Jizhong Depression. *Nat. Gas Ind.* **2018**, *38*, 33–42.
40. Du, J.; Zou, W.; Fei, B.; Lei, H.; Zhang, F.; Zhang, Y. *Buried Hill Oil and Gas Complex Zone in Jizhong Sub-Basin*; Petroleum Industry Press: Beijing, China, 2002.
41. Yang, K.; Dang, C.; Dai, F. Paleo-source/paleo-reservoir typed reservoirs: Cases of anticlinal paleo-reservoir and buried hill reservoirs in Bohaiwan Basin region. *Mar. Orig. Pet. Geol.* **2007**, *12*, 27–32.
42. Gao, X.; Wu, W.; Lu, X.; Cui, Z.; Kong, L.; Jia, L.; Wang, H. Multiplicity of hydrocarbon reservoir and accumulation controlling factors within buried hills in Jizhong depression. *J. China Univ. Pet.* **2011**, *35*, 31–35.
43. Yu, H.; Wang, D.; Niu, C.; Li, L. Characteristics and formation mechanisms of buried hill carbonate reservoirs in Bonan Low Uplift, Bohai Bay. *Pet. Geol. Exp.* **2015**, *37*, 150–156.
44. Chen, Q.; Lao, H.; Wu, K.; Wu, Z.; Cui, Y. Favorable hydrocarbon accumulation conditions for carbonate reservoirs in deep-buried hills in the Jizhong Depression, Bohai Bay Basin. *Nat. Gas Ind.* **2013**, *33*, 32–39.
45. Cilona, A.; Aydin, A.; Likerman, J.; Parker, B.; Cherry, J. Structural and statistical characterization of joints and multi-scale faults in an alternating sandstone and shale turbidite sequence at the Santa Susana Field Laboratory: Implications for their effects on groundwater flow and contaminant transport. *J. Struct. Geol.* **2016**, *85*, 95–114. [[CrossRef](#)]
46. Lai, J.; Li, D.; Wang, G.; Xiao, C.; Hao, X.; Luo, Q.; Lai, L.; Qin, Z. Earth stress and reservoir quality evaluation in high and steep structure: The Lower Cretaceous in the Kuqa Depression, Tarim Basin, China. *Mar. Pet. Geol.* **2019**, *101*, 43–54. [[CrossRef](#)]
47. Zeng, L.; Su, H.; Tang, X.; Peng, Y.; Gong, L. Fractured tight sandstone oil and gas reservoirs: A new play type in the Dongpu depression, Bohai Bay Basin, China. *AAPG Bull.* **2013**, *97*, 363–377. [[CrossRef](#)]
48. Milad, B.; Ghosh, S.; Suliman, M.; Slatt, R. Upscaled DFN Models to Understand the Effects of Natural Fracture Properties on Fluid Flow in the Hunton Group Tight Limestone. In Proceedings of the Unconventional Resources Technology Conference (URTeC), Houston, TX, USA, 23–25 July 2018.
49. Dashti, R.; Rahimpour-Bonaba, H.; Zeinali, M. Fracture and mechanical stratigraphy in naturally fractured carbonate reservoirs—A case study from Zagros region. *Mar. Pet. Geol.* **2018**, *97*, 466–479. [[CrossRef](#)]
50. Lyu, W.; Zeng, L.; Zhang, B.; Miao, F.; Lyu, P.; Dong, S. Influence of natural fractures on gas accumulation in the Upper Triassic tight gas sandstones in the northwestern Sichuan Basin, China. *Mar. Pet. Geol.* **2017**, *83*, 60–72. [[CrossRef](#)]
51. Liu, G.P.; Zeng, L.B.; Li, H.N.; Mehdi, O.; Minou, R. Natural fractures in metamorphic basement reservoirs in the Liaohe Basin, China. *Mar. Pet. Geol.* **2020**, *119*, 1–15. [[CrossRef](#)]
52. Ju, W.; Hou, G.; Feng, S.; Zhao, W.; Zhang, J.; You, Y.; Zhan, Y.; Yu, X. Quantitative prediction of the Yanchang Formation Chang 63 reservoir tectonic fracture in the Qingcheng-Heshui Area, Ordos Basin. *Earth Sci. Front.* **2014**, *21*, 310–320.
53. Liu, G.P.; Zeng, L.B.; Sun, G.; Zu, K.; Qin, L.; Mao, Z.; Mehdi, O. Natural fractures in tight gas volcanic reservoirs and their influences on production in the Xujiaweizi depression, Songliao Basin, China. *AAPG Bull.* **2020**. Available online: <http://archives.datapages.com/data/bulletns/aop/2020-06-22/aapgbtln17169aop.html> (accessed on 10 August 2020).
54. Gale, J.F.W.; Lander, R.H.; Reed, R.M.; Laubach, S.E. Modeling fracture porosity evolution in dolostone. *J. Struct. Geol.* **2010**, *32*, 1201–1211. [[CrossRef](#)]
55. Li, J.; Zeng, L.; Li, W.; Zhang, Y.; Cai, Z. Controls of the Himalayan deformation on hydrocarbon accumulation in the western Qaidam Basin, Northwest China. *China. J. Asian Earth Sci.* **2019**, *174*, 294–310. [[CrossRef](#)]
56. Dunham, J.B.; Larter, S. Association of Stylolitic Carbonates and Organic Matter: Implications for Temperature Control on Stylolite Formation. *AAPG Bull.* **1981**, *65*, 922.
57. Zeng, L.; Tang, X.; Wang, T.; Gong, L. The influence of fracture cements in tight Paleogene saline lacustrine carbonate reservoirs, western Qaidam Basin, northwest China. *AAPG Bull.* **2012**, *96*, 2003–2017. [[CrossRef](#)]
58. Dijk, P.E.; Berkowitz, B.; Yechieli, Y. Measurement and analysis of dissolution patterns in rock fractures. *Water Resour. Res.* **2002**, *38*, 1–12. [[CrossRef](#)]

59. Chaudhuri, A.; Rajaram, H.; Viswanathan, H. Alteration of fractures by precipitation and dissolution in gradient reaction environments: Computational results and stochastic analysis. *Water Resour. Res.* **2008**, *44*, 1–19. [[CrossRef](#)]
60. Rustichelli, A.; Tondi, E.; Agosta, F.; Cilona, A.; Giorgioni, M. Development and distribution of bed-parallel compaction bands and pressure solution seams in carbonates (Bolognano Formation, Majella Mountain, Italy). *J. Struct. Geol.* **2012**, *37*, 181–199. [[CrossRef](#)]
61. Göktan, R.M. Brittleness and micro-scale rock cutting efficiency. *Min. Sci. Technol.* **1991**, *13*, 237–241. [[CrossRef](#)]
62. Lorenz, J.C.; Sterling, J.L.; Schechter, D.S.; Whigham, C.L.; Jensen, J.L. Natural fractures in the Spraberry Formation, Midland Basin, Texas: The effects of mechanical stratigraphy on fracture variability and reservoir behavior. *AAPG Bull.* **2002**, *86*, 505–524.
63. Mavko, G.; Mukerji, T.; Dvorkin, J. *Elasticity and Hooke's Law in the Rock Physics Handbook*; Cambridge University Press: Cambridge, UK, 2009; pp. 169–228.
64. Zhang, C.; Dong, D.; Wang, Y.; Guan, Q. Brittleness evaluation of the Upper Ordovician Wufeng-Lower Silurian Longmaxi shale in southern Sichuan Basin, China. *Energy Explor. Exploit.* **2017**, *35*, 430–443. [[CrossRef](#)]
65. Bakri, Z.; Zaoui, A. Structural and mechanical properties of dolomite rock under high pressure conditions: A first-principles study. *Phys. Status Solid.* **2011**, *248*, 1894–1900. [[CrossRef](#)]
66. Zhao, X.; Hu, X.; Xiao, K.; Jia, Y. Characteristics and major control factors of natural fractures in carbonate reservoirs of Leikoupo Formation in Pengzhou area, western Sichuan Basin. *Oil Gas Geol.* **2018**, *39*, 30–39.
67. Laubach, E.S.; Olson, E.J.; Gross, R.M. Mechanical and fracture stratigraphy. *AAPG Bull.* **2009**, *93*, 1413–1426. [[CrossRef](#)]
68. McGinnis, N.R.; Ferrill, A.D.; Morris, P.A.; Smart, J.K. Mechanical stratigraphic controls on natural fracture spacing and penetration. *J. Struct. Geol.* **2017**, *95*, 160–170. [[CrossRef](#)]
69. Gillespie, P.A.; Howard, C.B.; Walsh, J.J.; Watterson, J. Measurement and characterization of spatial distributions of fractures. *Tectonophysics* **1993**, *226*, 113–141. [[CrossRef](#)]
70. Gross, M.R.; Fischer, M.P.; Engelder, T.; Greenfield, R.J. Factors controlling joint spacing in interbedded sedimentary rocks: Integrating numerical models with field observations from the Monterey formation, USA. *Geol. Soc. Lond. Spec. Publ.* **1995**, *92*, 215–233. [[CrossRef](#)]
71. Zhao, X.; Wang, Q.; Jin, F.; Wang, H.; Luo, J.; Zeng, J.; Fan, B. Main controlling factors and exploration practice of subtle buried-hill hydrocarbon reservoir in Jizhong depression. *Acta Pet. Sin.* **2012**, *33*, 71–79.
72. Gong, L.; Gao, S.; Fu, X.; Chen, S.; Lv, B.; Yao, J. Fracture characteristics and their effects on hydrocarbon migration and accumulation in tight volcanic reservoirs: A case study of the Xujiaweizi fault depression, Songliao Basin, China. *Interpretation* **2017**, *5*, 57–70. [[CrossRef](#)]
73. Qiao, H.; Fang, C.; Niu, J.; Guan, D. *Petroleum Geology of Deep Horizon in Bohaiwan Basin*; Petroleum Industry Press: Beijing, China, 2002.
74. Mattila, J.; Tammisto, E. Stress-controlled fluid flow in fractures at the site of a potential nuclear waste repository, Finland. *Geology* **2012**, *40*, 299–302. [[CrossRef](#)]
75. Zeng, L.; Li, X. Fractures in sandstone reservoirs with ultra-low permeability: A case study of the Upper Triassic Yanchang Formation in the Ordos Basin, China. *AAPG Bull.* **2009**, *93*, 461–477.

